Journal of Non-Newtonian Fluid Mechanics 310 (2022) 104921

Contents lists available at ScienceDirect

Journal of Non-Newtonian Fluid Mechanics

journal homepage: www.elsevier.com/locate/jnnfm

Pinch-off of bubbles in a polymer solution

Sreeram Rajesh *, Sumukh S. Peddada, Virgile Thiévenaz, Alban Sauret

Department of Mechanical Engineering, University of California, Santa Barbara, CA 93106, USA

ARTICLE INFO

Keywords:
Interfacial dynamics
Bubble
Pinch-off
Singularities
Polymer solution
Viscoelasticity

ABSTRACT

The formation of gas bubbles in a liquid occurs in various engineering processes, such as during foam generation or agitation and mixing in bubbly flows. A challenge in describing the initial formation of a gas bubble is due to the singular behavior at pinch-off. Past experiments in Newtonian fluids have shown that the minimum neck radius follows a power-law evolution shortly before the break-up. The exponent of the power-law depends on the viscosity of the surrounding Newtonian liquid, and ranges from 0.5 for low viscosity to 1 for large viscosity. However, bubble formation in a viscoelastic polymer solution remains unclear, and in particular, if the evolution is still captured by a power-law and how the exponent varies with the polymer concentration. In this study, we use high-speed imaging to analyze the bubble pinch-off in solutions of polymers. We characterize the time evolution of the neck radius when varying the polymer concentration and thus the characteristic relaxation time of the polymer chains, and describe the influence of viscoelasticity on the bubble pinch-off. Our results reveal that the presence of polymers does not influence the thinning until the latter stages, when their presence in sufficient concentration delays the pinch-off.

1. Introduction

Bubbles are encountered in a wide range of situations such as industrial processes [1], biological systems [2], and in geological studies [3]. In the medical industry, bubbles have been used as contrast agents for ultrasound scans [4]. Compound bubbles formed by water contaminated with harmful substances due to the possible aerosolization are of concern to our health [5–7]. Preventing cavitation bubbles is of crucial importance in biological networks in plants [8], or in the design of underwater turbines and propellers [9]. The formation of bubbles are also of particular interest in microfluidic devices [10], microcapillary tubes [11], as well as in turbulent flows [12]. In many applications, the liquids involved have a more complex rheology. For instance, the presence of cells, particles, or polymeric substances dispersed in the liquid modifies their rheology [13–21]. The modified rheology of polymer solutions has been exploited to achieve drag reduction in flow [22], and suppress the effect of cavitation [23]. It is known that the presence of polymers modifies the pinch-off of a liquid droplet in air [24,25]. The inverse problem of pinch-off of an air bubble in a polymer solution has received less attention.

The pinch-off of a gas bubble in a Newtonian liquid, shown in Fig. 1(a), is usually quantified through the time evolution of the minimum thickness $h_{\min}$ of the neck that connects the bubble with the nozzle. The moment t_c at which the bubble detaches from the nozzle in a Newtonian fluid is a singularity. For a short duration before the pinch-off, the minimum thickness follows a power law, $h_{\min}(t) \propto (t_c - t)^{\alpha}$. Burton et al. [26] have shown that the exponent α is a function of the external liquid viscosity for a Newtonian liquid. For inviscid liquids ($\eta \lesssim 10\,\mathrm{mPa\,s}$), the exponent is around 0.5 and for viscous liquids ($\eta \gtrsim 100\,\mathrm{mPa\,s}$), it is approximately 1. For liquids of intermediate viscosities, the exponent was reported in the range 0.5 to 1. A follow-up work by Thoroddsen et al. [27] at a higher spatial and temporal resolution reported an exponent of 0.57 for inviscid Newtonian liquids. This slightly larger exponent was theoretically derived by Eggers et al. as $\alpha = 1/2 + 1/[4\sqrt{-\ln(t_c - t)}]$ for the collapse of an axisymmetric cavity [28]. The exponents are hence non-universal, and depends on the initial condition of the system and the experimental resolution. In this study, we do not focus on the influence of the initial condition. Instead, we use a spatial and temporal resolution similar to Burton et al., which is sufficient to examine the moment leading up to the bubble pinch-off in polymer solutions. An example of thinning and pinch-off of a bubble in a polymer solution is shown in Fig. 1(b).

In the opposite configuration, *i.e.*, when a drop of inviscid liquid thins in air, the minimum thickness is described by the power-law $h_{\min}(t) \propto (t_c - t)^{2/3}$ [29]. Here, the time t_c describes the moment the drop separates from the liquid attached to the nozzle, as shown in Fig. 1(c). Until a time t_c, the thinning of polymer solution, shown in Fig. 1(d), is also captured by a power law [30]. At t_c, while the drop breaks off for a Newtonian liquid, adding even a small amount of polymer results

* Corresponding author.
E-mail addresses: sreeram@ucsb.edu (S. Rajesh), asauret@ucsb.edu (A. Sauret).

https://doi.org/10.1016/j.jnnfm.2022.104921
Received 27 May 2022; Received in revised form 13 September 2022; Accepted 17 September 2022
Available online 23 September 2022

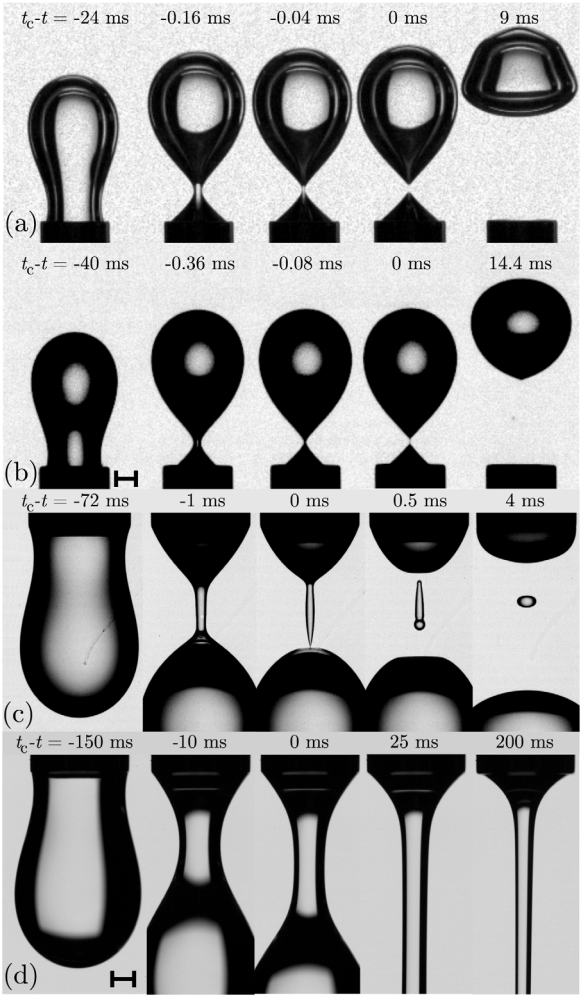

Fig. 1. Examples of a gas bubble pinch-off in a quiescent liquid of (a) 75/25% by weight water/glycerol, and (b) a polymer solution (0.5% mass concentration of 4000K PEO in 75/25% by weight water/glycerol). Examples of pinch-off in air of a liquid droplet of (c) 75/25% by weight water/glycerol (η_s = 2.14 mPas), and (d) a polymer solution (0.5% mass concentration of 4000K PEO in a 75/25% by weight water/glycerol). Scale bars are 1 mm.

in a transition to a viscoelastic thinning [24]. Microscopilcally, the transition corresponds to the unwinding of the polymer chains, which are initially present in a coiled state [30,31]. The uncoiled chains can interact with the flow and a macroscopic manifestation of this interaction is the formation of a long and slender liquid thread, which persists for a long time. A further consequence of polymer uncoiling is the increase in the flow resistance. When the polymers are coiled, their hydrodynamic interactions with the solvent are minimized. As the polymer unwinds, more regions of the chain are exposed to the solvent. This results in an increase in the viscosity of the solution, *i.e.*, an extensional thickening effect [24,32,33]. In this regime, the slender filament thins exponentially following $h_{\min}(t) \propto \exp[-t/(3\,\lambda_R)]$, where λ_R is the longest relaxation time of the polymer [34]. The exponential thinning is followed by either a beads-on-a-string (BOAS) instability [35], or a blistering instability [36].

While the pinch-off of bubbles in Newtonian liquids is well characterized [11,37], there is a dearth in the literature on bubble pinch-off in viscoelastic liquids. At a larger scale, notable differences exist for bubbles in viscoelastic liquids, such as the negative wake reported by Hassager [38]. The problem of discontinuity of the terminal velocity with respect to the bubble volume in polymer solutions has

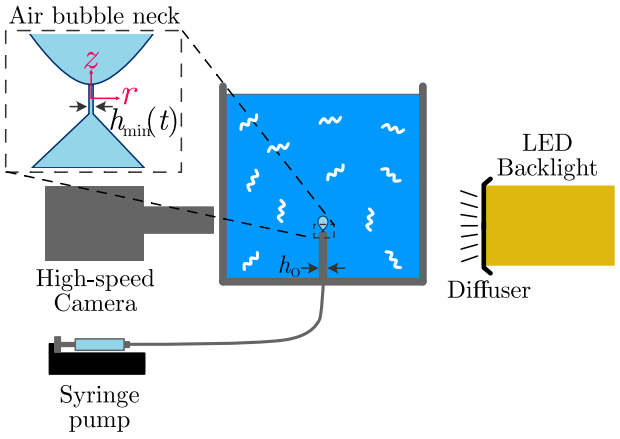

Fig. 2. Schematic of the experimental setup. A needle of internal diameter h_0 = 2.31 mm is set at the bottom of a tank filled with the liquid and connected to a syringe filled with air. A syringe pump is used to generate a bubble from the nozzle. The length h_{min} corresponds to the minimal thickness at the neck of the bubble. The z-axis corresponds to the axis of symmetry at the neck. The system is backlit with a LED (Light Emitting Diode) and a diffuser; the dynamics is recorded with a high-speed camera.

also been of long-standing interest [39,40]. The scales associated with the pinch-off are more challenging to capture and require a spatio-temporal resolution of a few microns over a few microseconds. A recent work by Jiang et al. [41] has reported the existence of two distinct regimes during the final stages of the bubble pinch-off in polymer solutions of higher concentrations. At lower polymer concentrations, the thinning is a power-law, with the exponent $0.5 < \alpha < 1$. This value is larger than the thinning exponent for the solvent, which is $\alpha = 0.5$. At higher concentrations, there is no clear description for the thinning. Yet, a recent study on the coalescence of two drops of liquid, which is another example of singular behavior [42], has shown that the minimum thickness of the coalescing polymer solutions is also described by a power-law and with the same exponent as the solvent [43]. The polymer solutions used in the coalescence study exhibit weak shear thinning and strong elasticity, *i.e.* a sufficiently large relaxation time. In contrast, the solutions used by Jiang et al. for their pinch-off experiments have strong shear thinning and elasticity for all the concentrations studied, with relaxation times of the order of a few seconds. In particular, the change in exponent observed by Jiang et al. [41] could be induced by the strong shear thinning of their solutions or the elastic effects, or by both.

To elucidate the influence of elasticity, we use polymer solutions that are weakly shear-thinning, except at large concentrations but with large enough relaxation times for all concentrations studied. The paper is organized as follows: in Section 2, we describe the experimental methods and the rheology of the polymer solutions used. We characterize the shear thinning and the relaxation time of the polymer solutions. In Section 3, we compare our results with Newtonian liquids to the results previously reported in the literature. We then present the thinning obtained for the polymer solutions. We observe that different concentrations of polymers lead to different pinch-off dynamics. We discuss our results in Section 4, where we describe the influence of elasticity on the shape of the bubble near the pinch-off. We further highlight this by presenting the contours of the bubble in the polymer solution as it breaks off.

2. Experimental methods

The bubble pinch-off experiments are performed in a 50×50×50 mm^3 transparent tank that contains the liquid (Fig. 2). A syringe pump (KDS Legato 110) extrudes air bubbles through a stainless-steel nozzle (inner diameter h_0 = 2.31 mm) at a controlled flow rate Q. The vertical

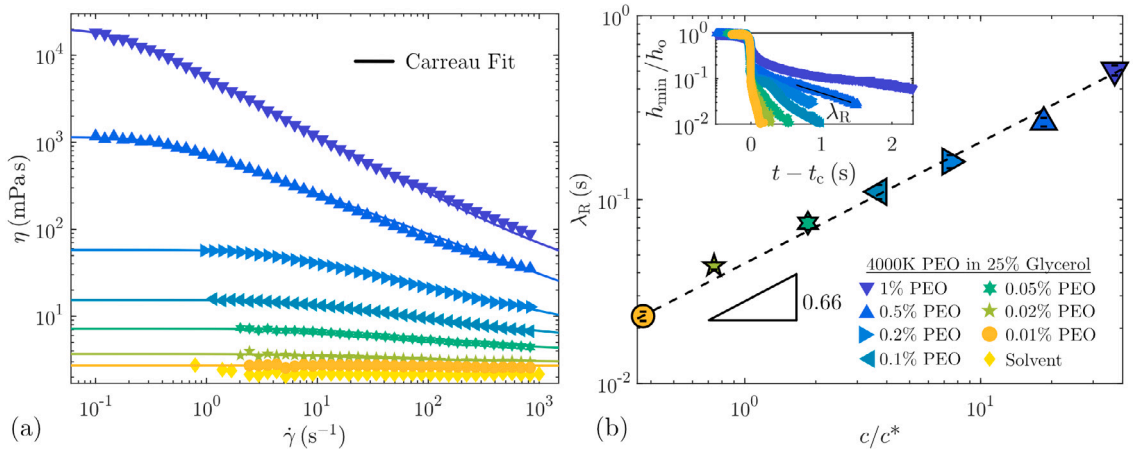

Fig. 3. Physical properties of the 4000K PEO polymer solutions with mass concentration between $c = 0.01\%$ and $c = 1\%$ prepared in a 75/25% by weight water/glycerol solvent. (a) Shear viscosity η of the solutions as a function of the shear rate $\dot{\gamma}$. (b) Relaxation time λ_R of the solutions measured from the droplet thinning experiments. The increase in the relaxation times with the concentration follows a power-law with an exponent 0.66. Inset: Thinning dynamics of PEO solutions. We extract the rescaled minimum thickness h_{min}/h_0 as a function of time. The relaxation time λ_R is obtained from the slope when $t - t_c > 0$, *i.e.*, after the transition to the viscoelastic regime.

alignment of the needle is obtained by using a custom 3D printed setup to place the needle in the tank. The tip of the needle is at least 10 mm below the air/liquid interface, ensuring that the free surface has no effect on the pinch-off dynamics. We use flow rates in the range $Q = 0.02\,\text{mL min}^{-1}$ to $0.2\,\text{mL min}^{-1}$ depending on the viscosity of the liquid. The flow rate is well below the critical flow rate where the flow transitions to jetting and allows to generate discrete bubbles in a quasi-static regime [44]. We ensure that changing the flow rate in this range does not influence the results, which confirms that we remain in a quasi-static regime (see supplementary materials).

The liquids consist of mixtures of deionized (DI) water and glycerol (Sigma-Aldrich) for the solvent, and the polymer solutions are prepared using Polyethylene oxide (PEO) of molecular weight $M_w = 4000\,\text{kg/mol}$ (Sigma Aldrich). We tune the viscosity of the solvent η_s by varying the weight fraction of glycerol from $\eta_s = 1\,\text{mPa s}$ (0% glycerol), to $\eta_s = 213.3\,\text{mPa s}$ (90% glycerol per weight). The change in the fraction of glycerol has minimal influence on the surface tension σ [45]. We prepare the polymer solutions by adding the polymer powder to a 75/25% by weight water/glycerol mixture, slowly mixing them on a roller mixer for 24–48 h, and we ensured that the polymer solutions are homogeneous at the end of the preparation. We use PEO of mass concentrations between $c = 0.01\%$ and $c = 1\%$. The surface tension, measured using the pendant drop method, does not vary significantly in this range of concentrations. The measurements are summarized in Table 1. An increase in the polymer concentration results in large variations of the shear viscosity η and the relaxation time λ_R. The shear viscosity is measured using a 50 mm 1° smooth cone-plate geometry on an MCR 302 rheometer (Anton Paar). We report the evolution of the shear viscosity with the shear rate $\dot{\gamma}$ in Fig. 3(a). We observe that up to a polymer concentration of approximately $c = 0.1\%$, the viscosity remains more or less constant, whereas the largest concentrations exhibit shear-thinning similar to observations reported in past studies [46]. The shear viscosity $\eta(\dot{\gamma})$ can be fitted using the Carreau model defined as $\eta = \eta_\infty + (\eta_0 - \eta_\infty)(1 + (\lambda\dot{\gamma})^2)^{\frac{n-1}{2}}$ [47]. The fitting parameters η_0, η_∞, λ, and n are the zero-shear viscosity, infinite shear viscosity, a time constant, and the power-law index, respectively. Their values are summarized in Table 1. The Carreau model was used to fit the viscosities instead of the Carreau-Yasuda model since it provided a more robust fit for all concentrations of polymer solutions used in the present study. While the Carreau-Yasuda model also fits the data well, it yields a larger error for $c = 1\%$ concentration due to a bias of the fitting model for the large viscosities measured at lower shear rates. In Fig. 3(b), we show

Table 1
Rheological properties and surface tension σ of the 75/25% by weight water/glycerol solvent, and PEO solutions of various mass concentrations ($c = 0.01\%$ to $c = 1\%$). $c^* = 0.291\,\text{kg/m}^3$ or 0.027% is the critical overlap mass concentration. λ_R is the longest relaxation time of the polymer. η_0, η_∞, λ, and n_{cf} are the parameters obtained from the Carreau fit shown in Fig. 3(a).

c	c/c^*	σ [mN/m]	λ_R [s]	η_0 [mPa s]	η_∞ [mPa s]	λ [s]	n_{cf}
0%	0	72.7	–	–	–	–	–
0.01%	0.37	62.3	0.023	2.7	1	0.041	1
0.02%	0.74	63.8	0.043	3.7	2.89	0.23	0.7
0.05%	1.85	63.8	0.074	7.2	3.02	0.2	0.8
0.1%	3.71	64.0	0.11	15.4	2.61	0.19	0.79
0.2%	7.41	63.8	0.16	57.9	0.52	0.36	0.72
0.5%	18.52	63.6	0.26	1150	0.1	2.63	0.54
1%	37.04	63.5	0.51	20000	18.5	6.78	0.32

the longest relaxation times λ_R of the polymer solutions, obtained from droplet pinch-off experiments [30,48]. We measure this relaxation time by fitting the rescaled minimum thickness h_{min}/h_0 during the formation of a liquid droplet in the viscoelastic regime ($t - t_c > 0$) with an exponential thinning model $h_{min} \propto e^{-(t-t_c)/3\lambda_R}$, as shown in the inset of Fig. 3(b) [34]. The relaxation time varies from $\lambda_R = 0.02\,\text{s}$ to $\lambda_R = 0.51\,\text{s}$ when increasing the PEO concentration from $c = 0.01\%$ to $c = 1\%$. The relaxation time was also measured from the relaxation modulus of the polymer solution for $c = 1\%$ concentration. The measured relaxation time was found to be comparable to the λ_R measured from droplet pinch-off [49], (see supplementary material) The evolution of the relaxation time with c is well captured by the empirical law $\lambda_R \propto (c/c^*)^{0.66}$ [25,48]. Here c^* is the critical overlap concentration above which the polymer coils starts to overlap. For the solutions used here, we calculate $c^* = 0.027\%$ [50].

We record the bubble pinch-off using a high-speed camera (Phantom VEO 710) equipped with a macro lens (Nikon Micro-NIKKOR 200 mm f/4 AI-s) and a microscope lens (Mitutoyo X2). The spatial resolution is about 10 µm per pixel. The recordings are typically made at 100,000 frames per second, and the setup is back-lit with an LED panel (GSVitec) with a diffuser. By repeating the experiments at other frame rates, we ensured that the power-law exponents are independent of the frame rates within the experimental resolution (see supplementary materials). We then process the recordings using custom ImageJ macros and Python routines to extract the temporal evolution of the minimum thickness h_{min} and outline of the bubble.

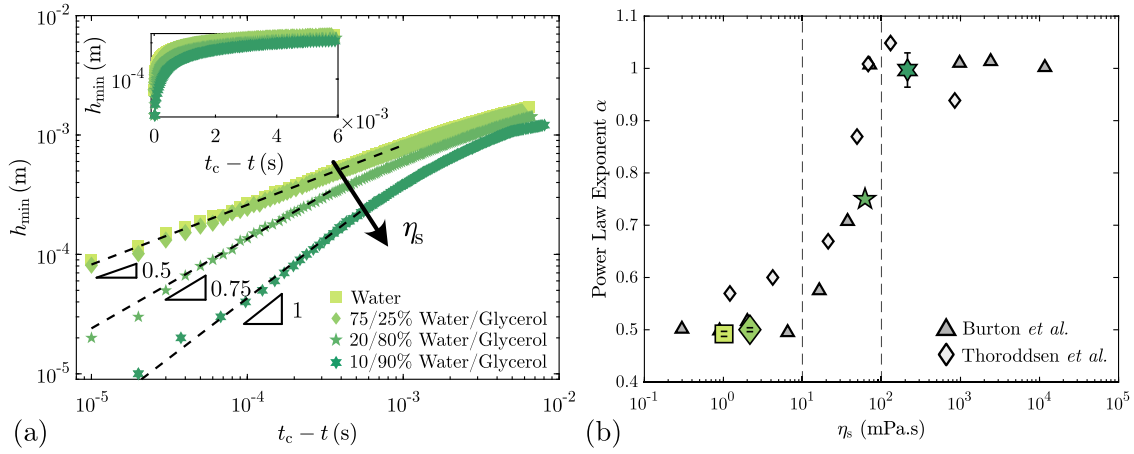

Fig. 4. Bubble pinch-off in Newtonian liquids. (a) Thinning dynamics for different Newtonian liquids: water (η_s = 1 mPa s) and mixture of water/glycerol at 75/25% by weight (η_s = 2.14 mPa s), 20/80% by weight (η_s = 62.1 mPa s), and 10/90% by weight (η_s = 213.3 mPa s). The pinch-off occurs at $t = t_c$, and the time goes from right to left. All experiments exhibit a power-law thinning before the pinch-off given by $h_{min} = A(t_c - t)^{\alpha}$. Inset: Semi-log plot of the temporal evolution of the minimum thickness for the same liquids. (b) Evolution of the power-law exponent α for air bubbles generated in Newtonian liquids of different shear viscosity. The viscosity is tuned by using water/glycerol mixtures with different compositions by weight of glycerol (between 0% and 90%). The exponents compare well with values previously reported in the literature (gray symbols) [26,27]. The two vertical lines delimit the regime at low viscosity ($\eta_s \leq$ 10 mPa s) where $\alpha \approx 0.5$ and at large viscosity where $\alpha \approx 1$ ($\eta_s \geq$ 100 mPa s).

3. Results

3.1. Bubble pinch-off in Newtonian fluids

Because of the short time scales involved in the pinch-off, finding the exact value of t_c is experimentally challenging. We can detect the last frame where the bubble is still connected to the nozzle and the first frame after the pinch-off, but cannot describe the thinning in between due to the limit of our temporal resolution (10 μs). We numerically improve this accuracy by searching for a best-fit power law in a narrow time range near t_c (see supplementary materials for more details) [43]. We test this method by comparing our measurements to the values in the literature for Newtonian solvents of different viscosities [26,27].

In Fig. 4(a), we report the time evolution of the minimum thickness h_{min} for the bubble in solvents with increasing fractions of glycerol, and hence, increasing viscosity. Because of the short timescale of the pinch-off, it is necessary to appropriately define t_c to recover the correct power-law exponent. Our experiments show that for all the viscosities, the resulting thinning dynamics are well-fitted with the equation $h_{min} = A(t_c - t)^{\alpha}$. For pure water and the 75/25% by weight water/glycerol solvent, which are in the inviscid limit (η_s < 10 mPas), the fitting parameters $\alpha \approx 0.5$ and $A \approx 0.025$ matches the results of Burton et al. [26]. In the viscous limit (η_s > 100 mPa s), the minimum thickness follows $h_{min} = (\sigma/\eta_s)(t_c - t)$ [51]. The experimental fit leads to $\alpha \approx 1$, similar to the exponents observed in previous studies [26,27]. For the prefactor, we recover $A \approx 0.4$, which is slightly larger than $\sigma/\eta_s = 0.34$ for the viscous solvent we use. We note a similar discrepancy in the data reported by Burton et al. [26]. For the 20/80% by weight water/glycerol solvent, which has an intermediate viscosity 10 mPa s < η_s < 100 mPa s, the fitting parameters are $\alpha \approx 0.75$, and $A \approx 0.135$. In Fig. 4(b), we summarize α and compare them with the exponents reported by Burton et al. [26] and Thoroddsen et al. [27]. The exponents we recover from our experimental method for the Newtonian solvents (mixture of water and glycerol) match the results observed in the literature. In the following, we consider the influence of viscoelasticity by adding polymers (PEO) to the solvent, and in particular, on the evolution of the thinning dynamics with the polymer concentration.

3.2. Bubble pinch-off in polymer solution

We now consider the formation of an air bubble in a viscoelastic solution of polymers. As shown in Figs. 1(c) and 1(d), the pinch-off of a drop of Newtonian liquid and a polymer solution in air are drastically different. Indeed, the thinning and pinch-off of a droplet of polymer solution in air exhibits two successive regimes [30]. First, a Newtonian regime where the thinning of the solution is similar to the solvent in which it was prepared, captured by $h_{min} \propto [\sigma(t_c - t)^2/\rho]^{1/3}$. Here t_c is the time at which the drop would have broken if there were no polymers dissolved [18,30]. The presence of polymers results in an increase in the extensional viscosity as the liquid thins, and delays the pinch-off [24]. Around $t = t_c$, the thinning slows down due to the coil-stretch transition of the polymers, and becomes viscoelastic [18,30]. The viscoelastic regime is characterized by a thread connecting the drop to the nozzle. This ligament thins exponentially as $h_{min} \propto e^{-t/(3\lambda_R)}$ where λ_R is the longest relaxation time of the polymer in the solvent [34].

For droplet pinch-off, the presence of polymer is felt even at very low concentrations, such as 0.001% or 10 parts per million by weight for solutions of a 4000K PEO [48]. Bubble pinch-off in polymer solution is different. In Figs. 5(a)–(b), we illustrate the thinning of an air bubble in polymer solutions of two different concentrations. Fig. 5(a) illustrates the formation of an air bubble in a solution of 4000K PEO at c = 0.01% and Fig. 5(b) at c = 1% mass concentration prepared in a 75/25% by weight water/glycerol solvent. For a certain duration of time, the thinning of the bubble appears similar in solutions of both low and high concentrations. At low polymer concentrations ($c \leq 0.02\%$), the bubble pinch-off is similar to the inviscid solvent. Following the definition for the solvents, the bubble detaches at time $t = t_c$. Above a certain concentration ($c \geq 0.05\%$), the pinch-off is modified; an air thread appears that binds the bubble to the nozzle (see supplementary materials). For bubbles in polymer solutions of concentration $c \geq 0.05\%$, we define $t = t_c$ as the moment when the thin and slender air thread first appears. This structure lasts for a very short time before the pinch-off. The thickness and lifetime of this structure increases with concentration, similar to the viscoelastic thinning of a drop in air. At the highest concentrations considered here (c = 0.5% and c = 1%), we have sufficient spatial and temporal resolutions to quantify this thinning, as shown in Fig. 6(a).

Similarly to the Newtonian liquid, we extract the time evolution of the minimum neck thickness h_{min} for polymer solutions of 4000K PEO of mass concentration 0.01% to 1% in Fig. 6(a). As noted before, and similar to the case of the pinch-off of a droplet of polymer solution in air [30], when the air thread appears, we define t_c as the time of its appearance, rather than the pinch-off time. While the difference is not strongly noticeable for dilute polymer solutions, the distinction must be made for larger concentrations (for solutions of $c \geq 0.05\%$). Indeed, for instance, for $c \geq 0.5\%$ of PEO, the pinch-off of the bubble

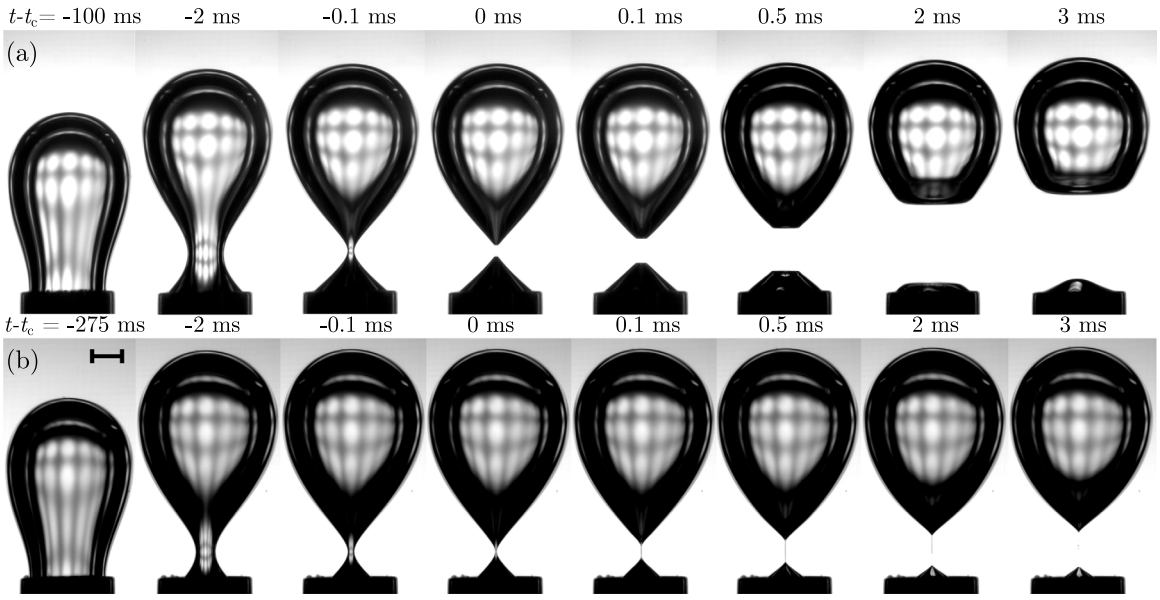

Fig. 5. Time sequence of bubble pinch-off in polymer solutions (a) in a $c = 0.01\%$ mass concentration of 4000K PEO in a 75/25% weight water/glycerol solvent and (b) in a $c = 1\%$ mass concentration of 4000K PEO in a 75/25% weight water/glycerol solvent. The scale bar is 1 mm.

only happens a few ms after the thread-like structure first appears. This is visible as a new regime of thinning in Fig. 6(a) when $t_c - t < 0$. Using the above criteria to select t_c, we report the time evolution of h_{min} in log–log scale in the inset of Fig. 6(a). Interestingly, all the polymer solutions considered in this study follows the same power law, $h_{min} = A(t - t_c)^{\alpha}$ with $\alpha = 0.496 \pm 0.01$. This result is remarkable, especially for solutions of higher concentrations, since the zero-shear viscosity of the solutions spans over four orders of magnitude. We further note that the prefactor $A \approx 0.025$ remains equal to that of the solvent, up to a concentration $c = 0.1\%$, and then decreases. This captures the slowing down of the thinning of the higher concentration solutions. We also draw attention to the thinning of the air thread when $t_c - t < 0$. At the highest concentrations we study ($c = 0.5\%$ and $c = 1\%$ mass concentration in 4000K PEO in 75/25% by weight water/glycerol solvent), we characterize the thinning using an exponential thinning model [34]. When $t_c - t < 0$, we define the minimum thickness as $h_{min} \propto e^{-(t_c - t)/(3\lambda_a)}$. Here, λ_a is a fitting parameter for the thinning of the air thread surrounded by a polymer solution, and is different from the relaxation time λ_R of the polymer solution. We estimate the values of this parameter as $\lambda_a \sim 0.027$ ms and $\lambda_a \sim 0.33$ ms for $c = 0.5\%$ and $c = 1\%$ concentrations, respectively. We note that the values are at least three orders of magnitude smaller than the relaxation times λ_R. This suggests that the pinch-off of a polymer drop in air and a gas bubble in a polymer solution, although are qualitatively similar in certain aspects, have notable differences.

4. Discussion

The thinning of a bubble in a polymer solution exhibits different behaviors depending on the solution concentration. However, by appropriately selecting t_c, we can extract the value of the power-law exponent α in the Newtonian regime. The log–log inset in Fig. 6(a) shows the evolution in the power-law regime for $c = 0.01\%$ to $c = 1\%$ mass concentration. We summarize the value of the exponent α when varying c in Fig. 6(b) and obtain $\alpha = 0.496 \pm 0.01$ for all polymer concentrations considered here. The results we report here, where the power-law exponent is independent of the polymer concentration, are similar to a recent study on the singular coalescence of polymer solutions [43]. For solutions that show weak shear thinning and strong viscoelasticity, similar to the solutions we use, the elastic coalescence also modifies the interface shape. As discussed later, we see a similar modification of the bubble interface near the pinch-off. Furthermore, the result is analogous to the droplet pinch-off of polymer solutions, where the Newtonian regime of the thinning has an exponent $\alpha = 2/3$ independent of the concentration [18,30]. We discuss two possible flow behavior of the surrounding polymer solutions during the bubble pinch-off to qualitatively rationalize why the exponent remains independent of the concentration. We assume that during the thinning, the liquid viscosity is either purely shear-thinning, or extensional thickening. In the inset of Fig. 6(b), we observe that the prefactor A, obtained from the best fit of a power-law, decreases with the polymer concentration, and has a sharp drop for $c = 1\%$ concentration. Similar observations have been made during the droplet thinning of solvents and suspensions of increasing viscosity [18]. Therefore, the prefactor can be considered as an amplitude of the second-order effect of viscosity on the thinning. This decrease in A and the observed slowing down of the thinning with increase in concentration suggests that the extensional thickening is a more likely mechanism at play here.

For the thinning shown in Fig. 6(a), we show the strain-rate $\dot{\epsilon}$ near the liquid/air interface in Fig. 7. The strain-rate scales as $\dot{\epsilon} \sim \dot{h}_{min}/h_{min}$ [24]. For the solvent and low concentration solutions, $\dot{\epsilon}$ diverges near t_c. At larger concentrations corresponding to the formation of the air thread, $\dot{\epsilon}$ reaches a maximal value near t_c and decreases when $t_c - t < 0$. This decrease is clearly visible for polymers concentrations of $c = 0.5\%$ and $c = 1\%$, where the experimental resolution allows us to track the thin air thread. In a shear flow, the polymer solutions are shear thinning, as shown in Fig. 3(a). If the solution shear thins, the thinning would become faster as we approach the pinch-off. However, the thinning slows down near the pinch-off in polymer solutions. A slower thinning suggests an increase in the flow resistance, similar to an extensional viscosity thickening in droplet pinch-off [24]. The increase in the flow resistance in the droplet pinch-off arises due to a coil-stretch transition when the flow reaches a critical strain rate [31]. Near $t \to t_c$, the strain-rate increases sharply, as shown in Fig. 7. Hence, it is likely that $\dot{\epsilon}(t_c - t \to 0)$ is large enough to uncoil the polymers in the vicinity of the liquid–air interface due to the local elongational flow. A macroscopic manifestation of the elastic interaction of the uncoiled polymers with the solvent is the modified interface shape we observe at larger concentrations, as can be seen when $t_c - t < 0$ in Fig. 5(b). When $t_c - t > 0$, far from the pinch-off, $\dot{\epsilon}$ is below the coil-stretch transition limit and the polymers do not interact with the flow [18,30]. The thinning depends only on the solvent, as suggested by Fig. 6(a) where the

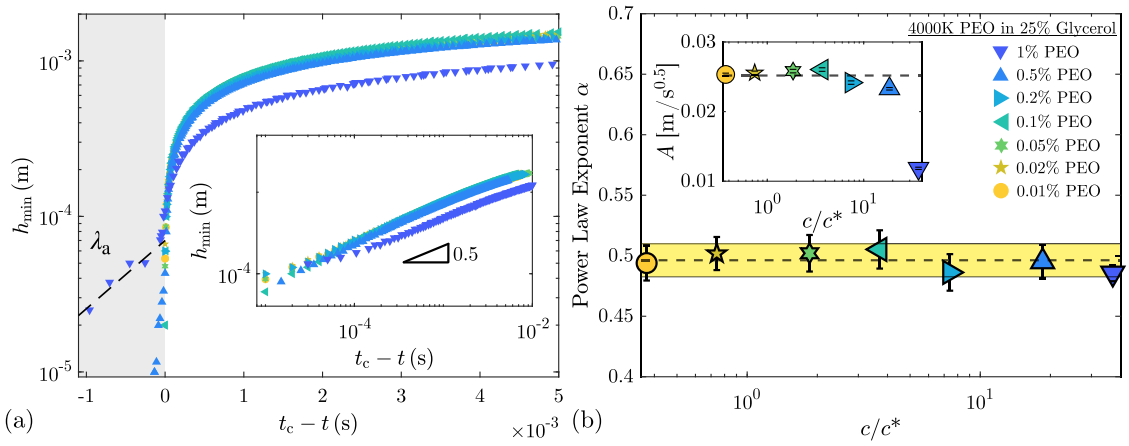

Fig. 6. Evolution of the minimum thickness h_{min} of an air bubble in a 4000K PEO solution at different concentrations c in a 75/25% by weight water/glycerol solvent. Note here that for solutions with a well-defined viscoelastic regime, t_c corresponds to the moment where the pinch-off would have occurred if there were no polymer in the solution. For $t_c - t < 0$, the thinning is fitted with an exponential thinning model with a fitting parameter λ_a. Inset: Log–log evolution of h_{min} for solutions of different concentrations. (b) Exponents α extracted from the power-law $h_{min} = A(t_c - t)^{\alpha}$ for the experiments performed in polymer solutions of different concentrations $c = 0.01\%$ to $c = 1\%$, with rescaled concentrations $c/c^* = 0.37$ to $c/c^* = 37$. The horizontal dashed line indicates the exponent $\alpha = 0.496 \pm 0.01$. The yellow shaded region is the standard deviation of the measured exponents. Inset: Evolution of the prefactor A with the polymer concentration.

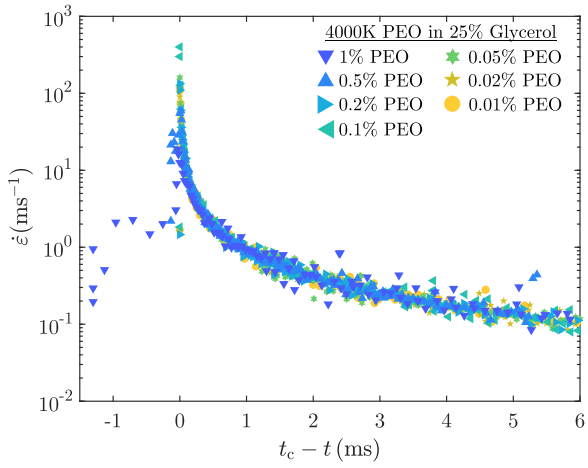

Fig. 7. Evolution of the strain-rate $\dot{\varepsilon}$ of the thinning for polymer solutions at different concentrations c. The strain rate reaches a maximum $\dot{\varepsilon}_{max}$ when the flow transitions from the Newtonian to the viscoelastic regime.

evolution of h_{min} for different polymer concentrations overlaps. This is further confirmed by the recovered exponents, which are independent of the polymer concentration. The slight difference observed at the highest concentration is associated with the increased viscosity due to the spherical polymer coils, following Einstein's laws [52].

When the strain-rate $\dot{\varepsilon}$ of the flow reaches its maximal value near $t = t_c$, the polymers likely start to uncoil locally near the interface. Further, the maximum coil-stretch transition strain-rate $\dot{\varepsilon}_{max}$ seems to decreases with the polymer concentration [30]. There are two possible explanations for why we see the air thread only above a threshold concentration. Indeed, it is likely that $\dot{\varepsilon}_{max}$ for the low concentration solutions ($c = 0.01\%$ and $c = 0.02\%$) is larger than the time resolution of our experiments, and the air thread thickness smaller than the lowest pixel length. Alternatively, the time scale of the singularity may be larger than the time scale of the coil-stretch transition strain-rate ($1/\dot{\varepsilon}_{max}$) of the solution, hence the bubble pinches off before it enters the viscoelastic regime.

The droplet and bubble pinch-off have similar features, such as a period of Newtonian power-law thinning, which is independent of the concentration, followed by a transition to a viscoelastic regime. However, we highlight certain key differences in the thinning, particularly during the viscoelastic regime. Although the air thread in the bubble pinch-off in polymer solutions resembles the viscoelastic filament in the droplet pinch-off, the thread itself has no polymers. The thinning of this thread is likely governed by the stretching of the polymers in the vicinity of the liquid/air interface. We recall that the air thread in the solutions with mass concentrations $c = 0.5\%$ and $c = 1\%$ have sufficient thickness to characterize their thinning. Although λ_a, the fitting parameter we obtain from the exponential thinning [34], resembles the relaxation time λ_R of the droplet thinning, they are at least three orders magnitude smaller. Further, the decrease in the prefactor A, shown in the inset of Fig. 6(b) implies that the thinning slows down with increase in the polymer concentration. We also estimate the time-scale of the stretching of the $c = 0.5\%$ and 1% polymer solutions during the bubble pinch-off as $1/\dot{\varepsilon}_{max} \sim 0.03$ ms. This gives an order of magnitude estimate of the extensional viscosity as $\eta = 2\sigma/(h_{min}\,\dot{\varepsilon}_{max}) \sim 80$ mPa s. It is also interesting to note that by rearranging the expression for the extensional viscosity $\eta = 2\sigma/(h_{min}\,\dot{\varepsilon}_{max})$ [24], we obtain $\tau_{\eta,c} \sim 1/\dot{\varepsilon}_{max}$, the visco-capillary time scale. The observations here is of an apparent paradox; even though the higher concentration solutions are more viscous, the exponent we recover is of an inviscid pinch-off.

Singularities in the bubble pinch-off are regions of topological transitions, where the initial bubble separates to form a main bubble and micron-sized satellite bubbles [53]. The differences in the topology arise either as a function of viscosity, illustrated in Figs. 8(a)–(d) or elasticity, which is the case in polymer solutions shown in Figs. 9(a)–(h). In Fig. 8(a), we show the bubble neck in a 75/25% by weight water/glycerol solvent before the pinch-off. The neck is fitted with a hyperbola of the form $r = R_1\sqrt{1+z^2}$, where r and z are the neck radius and the width, respectively, and R_1 is a fitting parameter. Similar fits have been considered for a bubble neck in an inviscid liquid in past literature [27]. Fig. 8(b) reports the spatial evolution of the neck for the time $t_c - t = 3$ to 0 ms using a polynomial fit. As the thinning approaches the singularity, we see the neck evolving from a smooth profile to a sharp corner before the pinch-off. When the bubble thins in a more viscous solvent, like the 10/90% water/glycerol shown in Fig. 8(c), the neck is modified. Viscosity has a smoothing effect on the neck, which is fitted with a parabola $r = az^2 + bz + c$, with a, b, and c as the fitting parameters. The parabolic neck has also been observed in previous studies [54]. Fig. 8(d) shows the polynomial fitted spatial neck profile a viscous liquid for $t_c - t = 3$ to 0 ms. In a viscous liquid, the neck has a smooth profile as it approaches the singularity.

For a bubble in polymer solutions, stretching of the polymers in the vicinity of the liquid/air interface results in an elastic contribution.

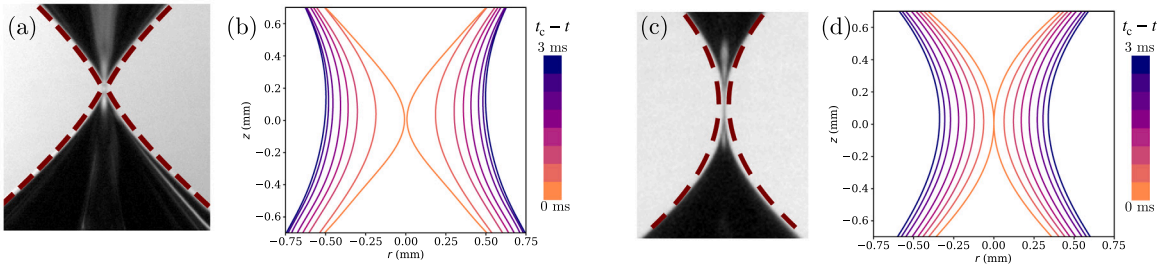

Fig. 8. Bubble neck profile and spatial evolution for Newtonian liquids. (a) Close-up view of the neck near the pinch-off in a 75/25% by weight water/glycerol (inviscid) solvent. The dotted lines at the liquid/air interface is a hyperbolic fit. (b) Polynomial fitted spatial evolution of the bubble in the corresponding solvent. (c) The bubble near the pinch-off in a 10/90% water/glycerol (viscous) solvent. The dotted line is a parabolic fit. (d) Polynomial fitted spatial evolution of the neck in the viscous solvent.

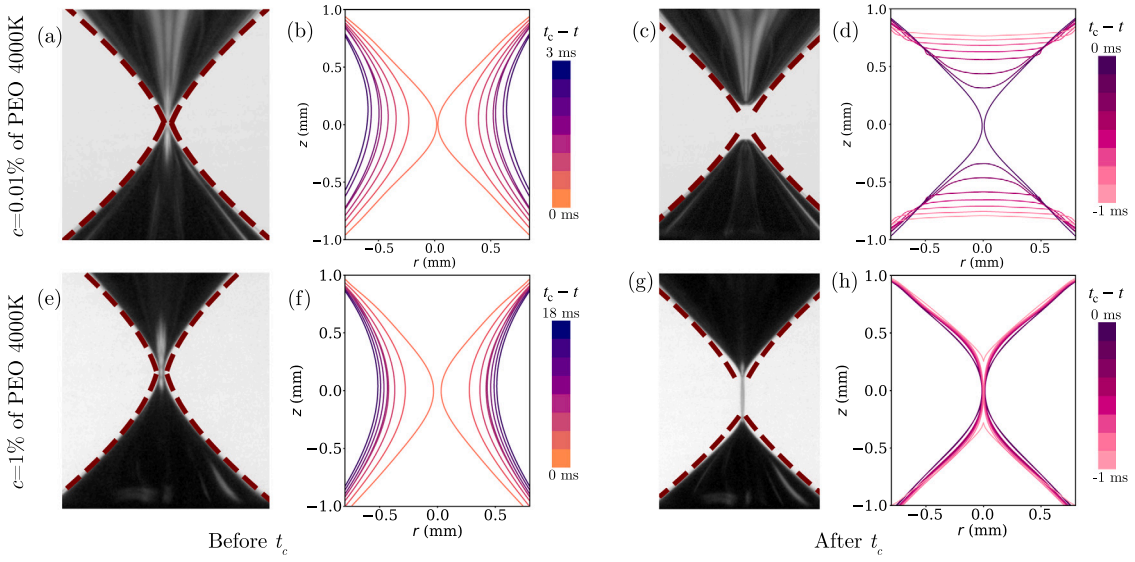

Fig. 9. Bubble neck profile and spatial evolution of the neck in a 4000K PEO solution in a 75/25% by weight water/glycerol solvent and (a)–(d) $c = 0.01\%$, (e)–(h) $c = 1\%$. (a) The bubble neck near the pinch-off, with a hyperbola fit. (b) Polynomial fitted spatial evolution of the neck near the pinch-off (c) The neck a μs after the pinch-off, with a hyperbolic fit. (d) Polynomial fitted spatial evolution of the neck after the pinch-off. (e) The bubble neck a few μs before the air thread forms at $t_c - t = 0$, fitted with a hyperbola. (f) Polynomial fitted spatial evolution of the neck before the air thread forms. (g) The bubble neck a μs after the pinch-off. The ends of the air thread is fitted with a hyperbola. (h) Polynomial fitted spatial evolution of the air thread.

At low concentrations, this contribution is likely beyond the limits of what we observe. Hence, the bubble neck profile for low polymer concentrations is similar to the bubble neck in the solvent. For a 0.01% mass concentration, we fit the neck near the pinch-off with a hyperbola as illustrated in Fig. 9(a). As reported in Fig. 9(b), the spatial evolution of the neck for the time $t_c - t = 3$ to 0 ms is also comparable to the solvent, which evolves at a similar rate. After the pinch-off, the hyperbolic neck in Fig. 9(c) destabilizes within a few milliseconds. We show this decay in Fig. 9(d). At a higher concentration, the local Deborah number $De \sim \lambda_R \dot{\epsilon}_{max}$ is of the order of 10^4. Thus, we expect the elastic forces to influence the bubble neck near the pinch-off. The solution is also more viscous due to a larger concentration of polymers. From a viscosity-based argument alone, we expect a smoother neck near the pinch-off for higher polymer concentration. However, the neck remains hyperbolic, as seen in a solution of 1% concentration in Fig. 9(e). We also note that as $t \to t_c$, the neck profiles are similar to the solvent and 0.01% solution. However, because of a larger viscosity of the solution, the neck evolves over a time $t_c - t = 18$ ms to 0 ms, as reported in Fig. 9(f). As discussed earlier, the dissolved polymers influence the thinning only when the strain-rate is sufficiently high. For $t_c - t < 0$, the elastic contribution modifies the neck to form the air thread visible in Fig. 9(g). Interestingly, we note that the neck, which connects the air thread, remains a hyperbola as the thread thins. Fig. 9(h) reports the fitted thinning of the neck. For $t_c - t < 0$, the elasticity strongly modifies the neck profile of the bubble. Hence, up to the point when the neck profile approaches $t = t_c$, the thinning depends only on the viscosity of the solvent. Elasticity begins to influence the thinning around $t = t_c$, which results in a unique bubble neck, different from the neck profiles reported for a bubble in inviscid and viscous liquids.

5. Conclusion

The pinch-off of a bubble is a classic example of singularities in fluids. As the bubble approaches pinch-off, the minimum thickness of the bubble neck follows a power-law. For a bubble in a Newtonian liquid, the power-law exponent α is a function of liquid density; it takes a value $\alpha \approx 0.5$ for low viscosity liquids and $\alpha \approx 1$ for high viscosity liquids. For a narrow range of viscosities in between, the exponent lies in the range $0.5 < \alpha < 1$. In this study, we consider the pinch-off of bubbles in polymer solutions of different concentrations. The solutions shows weak shear-thinning for the range of concentrations explored in this study, except at the highest concentrations, but produce strong viscoelastic effects in extensional flows at all concentrations. Further, the solutions have zero-shear viscosities varying over four orders of magnitude, and higher than that of the solvent. Thinning of the bubbles in low concentration polymer solutions (up to $c = 0.02\%$) is similar to that of the solvent. But for sufficiently high concentrations ($c \geq 0.05\%$), an air thread appears for a short time before the pinch-off. By defining an appropriate t_c, solutions of all concentrations follow a power-law

thinning with exponent $\alpha \approx 0.5$. Above a large enough concentration ($c > 0.5\%$ here), the spatio-temporal resolution of our experiments allows us to quantify the minimum thickness of the air thread. The thinning here indicates the existence of two distinct regimes before the pinch-off. Similar to the droplet pinch-off of polymer solutions in air [30], we define t_c not as the time when the bubble separates, but rather as when the thinning transitions from one regime to another. This approach allows us to show that the thinning of a bubble in polymer solutions of all concentrations we stduy also follows a power-law with an exponent $\alpha \approx 0.5$. The result is of notable interest as the solutions at larger concentrations are more viscous, yet the exponent remains inviscid. We attempt to rationalize this result by noting that near $t = t_c$, the thinning slows down. We identify a possible explaination for this observation as an increase in the viscosity of the solution near the pinch-off, similar to the extensional thickening observed during the droplet pinch-off of a polymer solution [24,30]. The increase in the viscosity is likely due to the unwinding of the polymers near the liquid/air interface at a critical strain-rate [31]. Until the point of coil-stretch transition, the polymer remains coiled and does not interact with the flow. This could explain why the exponent observed for the solutions remains similar to the solvent. The uncoiling and interaction of the polymers with the flow is macroscopically manifested as the unique cylindrical air thread formed by the bubble before it pinches off. The exponent observed also echoes the recent results obtained for the singular coalescence of polymer solution droplets, where a single exponent characterizes the power-law thinning independent of the concentration [43].

The strong elastic effects due to the high polymer concentrations lead to a change in the topology of the bubble near the pinch-off. For pinch-off in low viscosity Newtonian liquids, the neck of the bubble has a hyperbolic shape. Unlike the high viscosity solvents, which exhibit a parabolic neck, the polymer solutions retain the hyperbolic shape as they approach $t = t_c$. At sufficiently large concentration, the air thread structure becomes barely visible for a short time as a result of strong elastic forces experienced by the solution at high strain rates. At even higher concentrations, the effect on the topology of the air–liquid interface is evident. After a period of thinning during which the bubble has a hyperbolic shape and power-law thinning, it transitions to a regime with the elongated thread appearing, analogous to the cylindrical structure in the pinch-off of polymer drops.

Declaration of competing interest

The authors declare that they have no known competing financial interests or personal relationships that could have appeared to influence the work reported in this paper.

Data availability

Data will be made available on request.

Acknowledgments

This material is based upon work supported by the National Science Foundation, USA under NSF CAREER Program Award CBET Grant No. 1944844. The authors thank A. Pahlavan for helpful discussions.

Appendix A. Supplementary data

Supplementary material related to this article can be found online at https://doi.org/10.1016/j.jnnfm.2022.104921.

References

[1] Christopher Blair Crawford, Brian Quinn, 9 - microplastic separation techniques, in: Christopher Blair Crawford, Brian Quinn (Eds.), Microplastic Pollutants, Elsevier, 2017, pp. 203–218.
[2] Hugh D. Van Liew, Michael P. Hlastala, Influence of bubble size and blood perfusion on absorption of gas bubbles in tissues, Respir. Physiol. 7 (1) (1969) 111–121.
[3] A. Parmigiani, S. Faroughi, C. Huber, O. Bachmann, Y. Su, Bubble accumulation and its role in the evolution of magma reservoirs in the upper crust, Nature 532 (7600) (2016) 492–495.
[4] Martin J.K. Blomley, Jennifer C. Cooke, Evan C. Unger, Mark J. Monaghan, David O. Cosgrove, Microbubble contrast agents: a new era in ultrasound, BMJ 322 (7296) (2001) 1222–1225.
[5] Bingqiang Ji, Zhengyu Yang, Jie Feng, Oil-coated bubble formation from submerged coaxial orifices, Phys. Rev. Fluids 6 (3) (2021) 033602.
[6] Bingqiang Ji, Amrit Singh, Jie Feng, Oil column pinch-off controls the oil fraction of the oil-coated bubble, Phys. Fluids 33 (10) (2021) 103316.
[7] Bingqiang Ji, Zhengyu Yang, Jie Feng, Oil-coated bubble formation from submerged coaxial orifices, Phys. Rev. Fluids 6 (3) (2021) 033602.
[8] Timothy J. Brodribb, Diane Bienaimé, Philippe Marmottant, Revealing catastrophic failure of leaf networks under stress, Proc. Natl. Acad. Sci. 113 (17) (2016) 4865–4869.
[9] M.S. Plesset, The dynamics of cavitation bubbles, J. Appl. Mech. 16 (3) (1949) 277–282.
[10] Wim van Hoeve, Benjamin Dollet, Michel Versluis, Detlef Lohse, Microbubble formation and pinch-off scaling exponent in flow-focusing devices, Phys. Fluids 23 (9) (2011) 092001.
[11] Amir A. Pahlavan, Howard A. Stone, Gareth H. McKinley, Ruben Juanes, Restoring universality to the pinch-off of a bubble, Proc. Natl. Acad. Sci. 116 (28) (2019) 13780–13784.
[12] Daniel J. Ruth, Wouter Mostert, Stéphane Perrard, Luc Deike, Bubble pinch-off in turbulence, Proc. Natl. Acad. Sci. 116 (51) (2019) 25412–25417.
[13] Vincent A. Martinez, Jana Schwarz-Linek, Mathias Reufer, Laurence G. Wilson, Alexander N. Morozov, Wilson C.K. Poon, Flagellated bacterial motility in polymer solutions, Proc. Natl. Acad. Sci. 111 (50) (2014) 17771–17776.
[14] A.E. Patteson, A. Gopinath, M. Goulian, P.E. Arratia, Running and tumbling with E. coli in polymeric solutions, Sci. Rep. 5 (1) (2015) 15761.
[15] Shashank Kamdar, Seunghwan Shin, Premkumar Leishangthem, Lorraine F. Francis, Xinliang Xu, Xiang Cheng, The colloidal nature of complex fluids enhances bacterial motility, Nature 603 (7903) (2022) 819–823.
[16] Roy J. Furbank, Jeffrey F. Morris, An experimental study of particle effects on drop formation, Phys. Fluids 16 (5) (2004) 1777–1790.
[17] Virgile Thivénaz, Sreeram Rajesh, Alban Sauret, Droplet detachment and pinch-off of bidisperse particulate suspensions, Soft Matter 17 (2021) 6202–6211.
[18] Virgile Thiévenaz, Alban Sauret, Pinch-off of viscoelastic particulate suspensions, Phys. Rev. Fluids 6 (2021) L062301.
[19] Carina D.V. Martínez Narváez, Thomas Mazur, Vivek Sharma, Dynamics and extensional rheology of polymer–surfactant association complexes, Soft Matter 17 (2021) 6116–6126.
[20] Deok-Hoon Jeong, Michael Ka Ho Lee, Virgile Thiévenaz, Martin Z Bazant, Alban Sauret, Dip coating of bidisperse particulate suspensions, J. Fluid Mech. 936 (2022).
[21] Virgile Thiévenaz, Alban Sauret, The onset of heterogeneity in the pinch-off of suspension drops, Proc. Natl. Acad. Sci. 119 (13) (2022) e2120893119.
[22] Katepalli R. Sreenivasan, Christopher M. White, The onset of drag reduction by dilute polymer additives, and the maximum drag reduction asymptote, J. Fluid Mech. 409 (2000) 149–164.
[23] E.A. Brujan, C.-D. Ohl, W. Lauterborn, A. Philipp, Dynamics of laser-induced cavitation bubbles in polymer solutions, Acta Acust. United Acust. 82 (3) (1996) 423–430.
[24] Y. Amarouchene, D. Bonn, J. Meunier, H. Kellay, Inhibition of the finite-time singularity during droplet fission of a polymeric fluid, Phys. Rev. Lett. 86 (2001) 3558–3561.
[25] V. Tirtaatmadja, G.H. McKinley, J.J. Cooper-White, Drop formation and breakup of low viscosity elastic fluids: Effects of molecular weight and concentration, Phys. Fluids 18 (4) (2006) 043101.
[26] J.C. Burton, R. Waldrep, P. Taborek, Scaling and instabilities in bubble pinch-off, Phys. Rev. Lett. 94 (18) (2005) 184502.
[27] S.T. Thoroddsen, T.G. Etoh, K. Takehara, Experiments on bubble pinch-off, Phys. Fluids 19 (4) (2007) 042101.
[28] J. Eggers, M.A. Fontelos, D. Leppinen, J.H. Snoeijer, Theory of the collapsing axisymmetric cavity, Phys. Rev. Lett. 98 (9) (2007) 094502.
[29] Joseph B. Keller, Michael J. Miksis, Surface tension driven flows, SIAM J. Appl. Math. 43 (2) (1983) 268–277.
[30] Sreeram Rajesh, Virgile Thiévenaz, Alban Sauret, Transition to the viscoelastic regime in the thinning of polymer solutions, Soft Matter (2022).
[31] P.G. De Gennes, Coil-stretch transition of dilute flexible polymers under ultrahigh velocity gradients, J. Chem. Phys. (1974) 5030–5042.

[32] Jelena Dinic, Vivek Sharma, Macromolecular relaxation, strain, and extensibility determine elastocapillary thinning and extensional viscosity of polymer solutions, Proc. Natl. Acad. Sci. 116 (18) (2019) 8766–8774.
[33] Jelena Dinic, Yiran Zhang, Leidy Nallely Jimenez, Vivek Sharma, Extensional relaxation times of dilute, aqueous polymer solutions, ACS Macro Lett. 4 (7) (2015) 804–808.
[34] Shelley L. Anna, Gareth H. McKinley, Elasto-capillary thinning and breakup of model elastic liquids, J. Rheol. 45 (2001) 115–138.
[35] Christian Clasen, Jens Eggers, Marco A. Fontelos, Jie Li, Gareth H. McKinley, The beads-on-string structure of viscoelastic threads, J. Fluid Mech. 556 (2006) 283–308.
[36] A. Deblais, K.P. Velikov, D. Bonn, Pearling instabilities of a viscoelastic thread, Phys. Rev. Lett. 120 (2018) 194501.
[37] Raymond Bergmann, Anders Andersen, Devaraj van der Meer, Tomas Bohr, Bubble pinch-off in a rotating flow, Phys. Rev. Lett. 102 (2009) 204501.
[38] Ole Hassager, Negative wake behind bubbles in non-newtonian liquids, Nature 279 (5712) (1979) 402–403.
[39] L.G. Leal, J. Skoog, A. Acrivos, On the motion of gas bubbles in a viscoelastic liquid, Can. J. Chem. Eng. 49 (5) (1971) 569–575.
[40] Dieter Bothe, Matthias Niethammer, Christian Pilz, Günter Brenn, On the molecular mechanism behind the bubble rise velocity jump discontinuity in viscoelastic liquids, J. Non-Newton. Fluid Mech. 302 (2022) 104748.
[41] Xiao F. Jiang, Chunying Zhu, Huai Z. Li, Bubble pinch-off in Newtonian and non-Newtonian fluids, Chem. Eng. Sci. 170 (2017) 98–104.
[42] Joseph D. Paulsen, Rémi Carmigniani, Anerudh Kannan, Justin C. Burton, Sidney R. Nagel, Coalescence of bubbles and drops in an outer fluid, Nature Commun. 5 (1) (2014) 1–7.
[43] Pim J. Dekker, Michiel A. Hack, Walter Tewes, Charu Datt, Ambre Bouillant, Jacco H. Snoeijer, When elasticity affects drop coalescence, Phys. Rev. Lett. 128 (2) (2022) 028004.
[44] Hasan N. Oguz, Andrea Prosperetti, Dynamics of bubble growth and detachment from a needle, J. Fluid Mech. 257 (-1) (1993) 111.
[45] Koichi Takamura, Herbert Fischer, Norman R. Morrow, Physical properties of aqueous glycerol solutions, J. Pet. Sci. Eng. 98–99 (2012) 50–60.
[46] Pim J. Dekker, Michiel A. Hack, Walter Tewes, Charu Datt, Ambre Bouillant, Jacco H. Snoeijer, Supplementary material for 'when elasticity affects drop coalescence', Phys. Rev. Lett. (2022) 7.
[47] R. Byron Bird, Robert C. Armstrong, Ole Hassager, Dynamics of Polymeric Liquids, Volume 1: Fluid Mechanics, second ed., Wiley, 1987, pp. 210–211.
[48] A. Deblais, M.A. Herrada, J. Eggers, D. Bonn, Self-similarity in the breakup of very dilute viscoelastic solutions, J. Fluid Mech. (2020) R2.
[49] Sarath Chandra Varma, Abhineet Singh Rajput, Aloke Kumar, Rheocoalescence: Relaxation time through coalescence of droplets, Macromolecules (2022).
[50] William W. Graessley, Polymer chain dimensions and the dependence of viscoelastic properties on concentration, molecular weight and solvent power, Polymer 21 (3) (1980) 258–262.
[51] J. Eggers, Singularities at interfaces, in: Soft Interfaces, Oxford University Press, Oxford, 2017.
[52] E.W.J. Mardles, Viscosity of suspensions and the Einstein equation, Nature 145 (3686) (1940) 970.
[53] J.M. Gordillo, M.A. Fontelos, Satellites in the inviscid breakup of bubbles, Phys. Rev. Lett. 98 (2007) 144503.
[54] R. Bolaños-Jiménez, A. Sevilla, C. Martínez-Bazán, D. van der Meer, J.M. Gordillo, The effect of liquid viscosity on bubble pinch-off, Phys. Fluids 21 (7) (2009) 072103.